Angle-resolved photoemission spectral function analysis of the electron-doped cuprate $Nd_{1.85}Ce_{0.15}CuO_4$

N. P. Armitage,[1,2,3] D. H. Lu,[3] C. Kim,[3] A. Damascelli,[3,4] K. M. Shen,[3,4] F. Ronning,[2,3] D. L. Feng,[2,3] P. Bogdanov,[3,4] X. J. Zhou,[3,5] W. L. Yang,[5] Z. Hussain,[5] P. K. Mang,[3,4] N. Kaneko,[3,4] M. Greven,[3,4] Y. Onose,[6] Y. Taguchi,[6] Y. Tokura,[6] and Z.-X. Shen[2,3,4]

[1]*Department of Physics and Astronomy, University of California, Los Angeles, California 90095, USA*
[2]*Department of Physics, Stanford University, Stanford, California 94305, USA*
[3]*Stanford Synchrotron Radiation Laboratory, Stanford University, Stanford, California 94305, USA*
[4]*Department of Applied Physics, Stanford University, Stanford, California 94305, USA*
[5]*Advanced Light Source, Lawrence Berkeley National Laboratory, Berkeley, California 94720, USA*
[6]*Department of Applied Physics, The University of Tokyo, Tokyo 113-8656, Japan*

Using methods made possible by recent advances in photoemission technology, we perform an indepth line shape analysis of the angle-resolved photoemission spectra of the electron doped (*n*-type) cuprate superconductor $Nd_{1.85}Ce_{0.15}CuO_4$. Unlike for the *p*-type materials, we only observe weak mass renormalizations near 50–70 meV. This may be indicative of smaller electron-phonon coupling or due to the masking effects of other interactions that make the electron-phonon coupling harder to detect. This latter scenario may suggest limitations of the spectral function analysis in extracting electronic self-energies when some of the interactions are highly momentum dependent.

I. INTRODUCTION

Angle-resolved photoemission spectroscopy (ARPES) is one of the most direct probes of the electronic structure of solids. In recent years, with the advent of *Scienta* analyzers and high-flux beam lines, a new era of photoemission line shape analysis has been ushered in.[1,2] The advances offer unprecedentedly high momentum and energy resolution, as well as the ability to do simultaneous parallel angle scanning and thereby generate direct two-dimensional (2D) $E-\vec{k}$ images of ARPES spectral functions. Whereas, ARPES data have been displayed traditionally as energy distribution curves (EDC's) in which the photoemission intensity is plotted as a function of energy at specific angles, now they can be represented in terms of these detailed 2D intensity plots, and in analogy with EDC's, complementary momentum distribution curves (MDC's) can be generated. Such advances are making new analysis methods possible, where one is able to bring to bear the considerable mathematical machinery of many-body physics for intuition and interpretation.

Within the sudden approximation, ARPES measures the single-particle spectral function $A(\vec{k},\omega)$.[1–3] Assuming that the material under investigation has well-defined electronic excitations,[4] the single-particle spectral function can be represented compactly in terms of a complex self-energy $\Sigma = \Sigma' + i\Sigma''$ as

$$A(\vec{k},\omega) = \frac{1}{\pi} \frac{\Sigma''(\vec{k},\omega)}{[\omega - \epsilon_{\vec{k}} - \Sigma'(\vec{k},\omega)]^2 + [\Sigma''(\vec{k},\omega)]^2}. \quad (1)$$

In momentum regions where $\Sigma(\vec{k},\omega)$ is a weak function of $\vec{k}$ and the bare dispersion can be linearized as $\epsilon_{\vec{k}} = \vec{v}_F^0 \cdot (\vec{k} - \vec{k}_F)$ (where $\vec{v}_F^0$ is the bare band velocity), $A(\vec{k},\omega)$ at constant ω can be put in the form of a Lorentzian centered at $\omega/\vec{v}_F^0 + k_F - \Sigma'(\vec{k},\omega)/\vec{v}_F^0$ with width $\Sigma''(\vec{k},\omega)/\vec{v}_F^0$.

Fits to MDC's gives one, in principle, not only a measure of $\Sigma''(\vec{k},\omega)$, but also a more accurate parametrization of the renormalized dispersion in the case of a rapidly changing $\Sigma'(\vec{k},\omega)$. Such an analysis allows one to probe the dominant kinds of electron-electron interactions as well as for signatures of electronic interaction with bosonic modes. Such studies are an area of much current focus in the ARPES community with, for instance, the observation of bosonic effects in the ARPES spectra of systems with strong electron-phonon coupling such as Be and Mo.[6–8] Recently, similar features have been found in the low-energy ARPES spectra of a number of high-temperature hole doped cuprate superconductors. A mass renormalization, or "kink," in the dispersion has been found ubiquitously in the *p*-type materials (at ≈ 70 meV);[9,10] its origin is a matter of much current debate. Some groups have pointed to a many-body electronic source[11–13] that is perhaps related to the magnetic resonance mode discovered *via* neutron scattering. However, this assignment has been disputed on the grounds that the resonant mode may have insufficient spectral weight to cause the observed effect with reasonable estimates for its coupling strength.[14,15] Others have argued that the kink's presence above T_c and its universality among material classes demonstrate a phononic origin and indicate the strong role that lattice effects have on the low-energy physics.[10]

Although, in principle, it is straightforward with the above analysis to extract the electronic self-energy from ARPES spectra, it is not as obvious how to assign parts of the self-energy to different origins. For instance, is the phenomenon that causes the kink the same one that causes the pseudogap in the underdoped materials, or are multiple effects playing a role? Moreover, there have even been reports that distinguish

the kinks near the $(\pi,0)$ and $(\pi/2,\pi/2)$ positions.[13] Similar manifestations of the various phononic, antiferromagnetic, charge order, stripe, and structural effects (not to mention the possibility of hidden orders[16]) that may exist in the cuprates make it difficult to extract unambiguous information from a spectral function analysis.

Such problems may be particularly acute in the electron doped system $Nd_{2-x}Ce_xCuO_4$.[17] In previous ARPES work on the "optimally-doped" ($x=0.15$) system, high-energy pseudogap effects (i.e., the suppression of low-energy spectral weight over an extended frequency range) similar to those in the underdoped p-type compounds were observed.[18,19] However, unlike in the p-type compounds, these regions of maximum pseudogap were not on the Fermi surface (FS) near $(\pi,0)$ (the maximum of the $d_{x^2-y^2}$ functional form), but instead at "hot-spots" at the intersection of the FS with the antiferromagnetic Brillouin zone (BZ) boundary.[18] This, along with the fact that the antiferromagnetic and superconducting phases in the highest T_c samples ($x=0.15$) are in very close proximity to each other and may in fact coexist,[20] led to the conclusion that this high-energy pseudogap was due to the effects of antiferromagnetic or other orders with characteristic wave vector (π,π).[18] As the signatures of boson-electron interactions are somewhat generic, it may be difficult to distinguish interactions with different types of modes (for instance phonons vs spin fluctuations) if the regions of the BZ, where such effects are observed to be the strongest, overlap. In the context of Eq. (1), this raises the question of the $\vec{k}$-independence of the self-energy implied in this type of analysis, especially in the n-type materials where the momentum-dependent scattering appears to be very strong even near optimal doping.[18]

Keeping the above considerations in mind, we present an ARPES line-shape analysis of the electron doped (n-type) cuprate superconductor $Nd_{1.85}Ce_{0.15}CuO_4$. We use essentially the same methodologies that have been employed in the study of p-type compounds as we believe that a direct comparison has utility despite the fact that there may be possible complications. We find that there is no kink along the zone diagonal, in contrast to the p-type materials where this is the region of the BZ where it can be most unambiguously identified. In the $(\pi,0)$ to (π,π) direction, a very weak kink in the quasiparticle dispersion can be found. However, it is not straightforward to identify this effect with phonons since competing effects cannot be separated unambiguously in this region of the BZ. Despite an apparent lack of a mass renormalization along the zone diagonal, a very slight drop in the scattering rate is observed in this direction. No such drop in the scattering rate is observed near the $(\pi,0)$ to (π,π) FS crossing. As it is reasonable that this class of many-body effects along the nodal direction in the p-type compounds can be identified with effects of phonons, the lack of a kink and weak drop in the scattering rate along the same direction indicates a weaker electron-phonon interaction in $Nd_{1.85}Ce_{0.15}CuO_4$.

II. EXPERIMENT

Angle-resolved photoemission data were recorded at beam line 10.0.1.1 of the Advanced Light Source with a photon energy of 55 eV in a glancing-incidence geometry. The polarization angles were 45° to the Cu-O bonds for the Γ to (π,π) cut and along the Cu-O bonds for the $(\pi,0)$ to (π,π) cut. The energy resolution was typically 18 meV and angular resolution was 0.14° (corresponding to $\approx 0.5\%$ of the Brillouin zone size). This configuration is identical to that used in an extensive study of the kink in the hole doped compounds.[10] The samples were cleaved *in situ* at low temperatures in vacuum better than at 4×10^{-11} Torr. As there are only minor changes to the spectra when entering the superconducting state,[19] all displayed spectra were taken at low temperature (≈ 15–25 K). No signs of surface aging were seen for the duration of the experiment (≈ 24 h). In addition to the displayed data, extensive measurements were performed on beam line 5-4 of the Stanford Synchrotron Radiation Laboratory; results were obtained that are consistent with those displayed here.

Single crystals of $Nd_{1.85}Ce_{0.15}CuO_4$ were grown by the traveling-solvent grown method in 4 atm of O_2. The as-grown crystals are not superconducting and must be annealed to remove excess apical oxygen. The displayed data come from samples that were heated in flowing argon gas for 20 h at 920 °C and then a further 20 h at 500 °C under pure O_2.[21] Resistivity and magnetic susceptibility measurements show an onset of the superconducting transition at 24 K.

III. RESULTS

In Fig. 1, we show the raw data in the form of 2D intensity plots of the spectral function, along with the corresponding EDC's for $\vec{k}$-space cuts, in the Γ to (π,π) and the $(\pi,0)$ to (π,π) directions. In Fig. 2, we show the same data represented in a more traditional fashion with EDC's selected at larger angular intervals (0.5°). In the Γ to (π,π) direction, a large broad feature disperses out of the background, sharpens to a peak at E_F, and then disappears. As pointed out previously,[18] this is behavior not unlike that found in optimally doped p-type compounds. In the $(\pi,0)$ to (π,π) direction, an almost parabolic-shaped band centered around $(\pi,0)$ is observed. A similar sharpening of the feature as it disperses to E_F is seen here as well, however, the $|\vec{k}|<|\vec{k}_F|$ EDC's seem to show additional structure in the form of two separate peaks. This aspect has been also noted previously.[18,19,22]

The MDC's from the raw false intensity plots in Figs. 1(a) and 1(c) were fitted to Lorentzians as detailed above. Representative fits are shown in Fig. 3 at $\omega=0$ and $\omega=150$ meV slices. At energies higher than those displayed, the MDC line-shape begins to differ more significantly from a simple Lorentzian.

At the displayed relevant lower energies, the Lorentzian functional forms fit the MDC's relatively well, showing that, although there may be large momentum dependence in the self-energy in other parts of the BZ, the changes across the displayed regions are minimal at low energy. The fact that the fits begin to break down at higher energies indicates that momentum dependent effects may become relevant. These fits to the position are displayed in Fig. 4 with the corre-
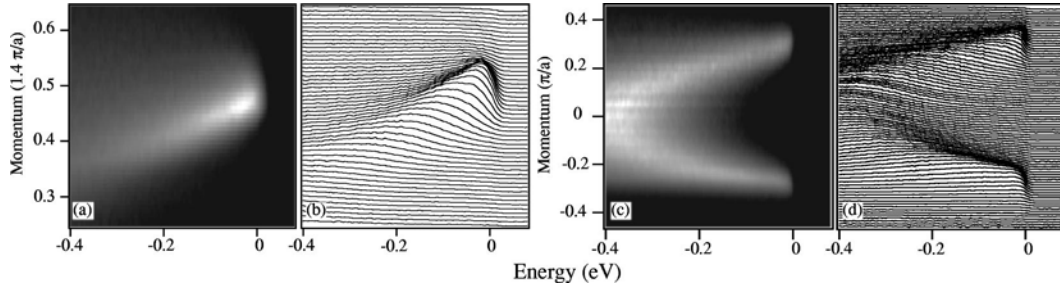
FIG. 1. Data from high-symmetry directions with $E_\gamma = 55$ eV. (a) Image of the spectral function along the Γ to (π, π) direction. (b) EDC's from (a). (c) Image of the spectral function along the $(\pi, -\pi)$ to (π, π) direction. (d) EDC's from (c). The lower piece of the parabola in (c) is slightly distorted from its intrinsic shape as these data were at the edge of the detector multichannel plate and were likely affected by astigmatism in the electron lens.

sponding energy widths Σ'' shown in Fig. 5. Horizontal and vertical errorbars in the Figs. 4 and 5, respectively, represent the uncertainties in the values from the Lorentzian fits. In Fig 4(a), we show the dispersion along the zone diagonal plotted from the momentum space peak position. As seen by comparison with the linear fit, there is only a gentle slope change and no sign of a sharp mass renormalization at low energy. This is in sharp contrast to the p-type materials where this is the region of the BZ that shows the most unambiguous effect at ≈ 70 meV.

The behavior along the $(\pi, 0)$-(π, π) direction differs from that of the zone diagonal. Here, the smooth dispersion deviates at low energy from the parabolic fit in the region indicated by the arrow in Fig. 4(b). The deviation in the dispersion is greater than the uncertainty in the fit. The small mass renormalization around 55 meV has the same energy scale as the dip structure in the EDC in Fig. 2. This is close to the same energy scale as the mass renormalization onset in the p-type compounds. If one is to identify this apparent mass change with coupling to a bosonic mode, a simple

analysis for the dimensionless coupling parameter λ' $= \vec{v}_F^0 / v_F - 1$ gives a value $\lambda' \approx 0.3$. This may be compared with values ≈ 0.5 extracted via the same method from the zone diagonal direction of the p-type materials near optimal doping.[23] In this simple analysis, we used as a value for $\vec{v}_F^0$ the velocity from the dispersion above the expected kink energy and the $\vec{v}_F$ from a low ω fit, as was done in the analysis for the p-type materials.[10]

Closer to the spirit of how a mass renormalization is typically defined would be to use a $\omega \rightarrow 0$ extrapolation of a function fitted to the dispersion at higher energy ($\omega > 100$ meV). Analyzing the data in this fashion gives velocities of $\vec{v}_F^{0eff}(\omega \rightarrow 0) = 4.3 \times 10^5$ m/sec$[(2.3 \text{ eV})a/\hbar\pi]$ for the Γ-(π, π) FS crossing and $\vec{v}_F^{0eff}(\omega \rightarrow 0) = 3.4 \times 10^5$ m/sec$[(1.8 \text{ eV})a/\hbar\pi]$ for the $(\pi, 0)$-(π, π) FS crossing. Using this value for v_F^0 for the $(\pi, 0)$-(π, π) cut gives a smaller λ' of ≈ 0.1. However, the values for λ' near $(\pi, 0)$ arrived at in this fashion are not readily comparable to those of the hole doped compounds along the zone diagonal as their dispersion there does not appear to recover to something resembling an unrenormalized dispersion within the experimental window. This is most likely a consequence of
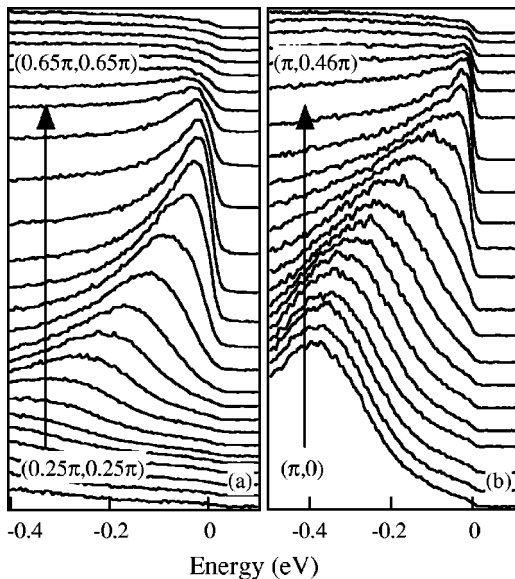

FIG. 2. $E_\gamma = 55$ eV EDC's representing the data of Fig. 1 in a more traditional fashion. (a) $(0.25\pi, 0.25\pi) \rightarrow (0.65\pi, 0.65\pi)$. (b) $(\pi, 0) \rightarrow (\pi, 0.46\pi)$. The EDC's are offset for clarity.
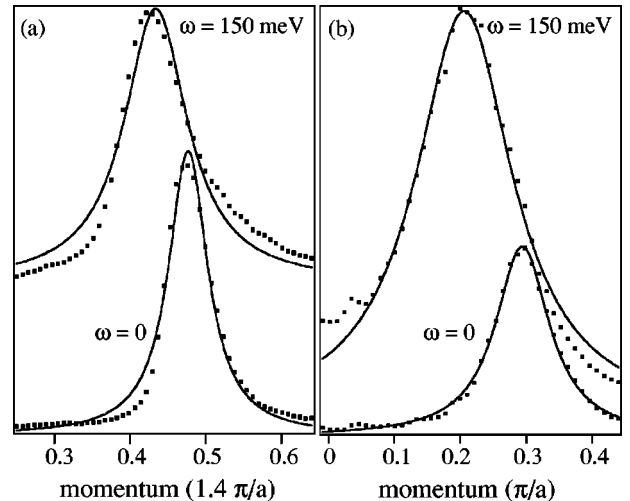

FIG. 3. MDC's from Fig. 1 at $\omega = 0$ and $\omega = 150$ meV binding energy along the two main symmetry directions. (a) $\Gamma \rightarrow (\pi, \pi)$, (b) $(\pi, 0) \rightarrow (\pi, \pi)$. The spectra are offset for clarity.
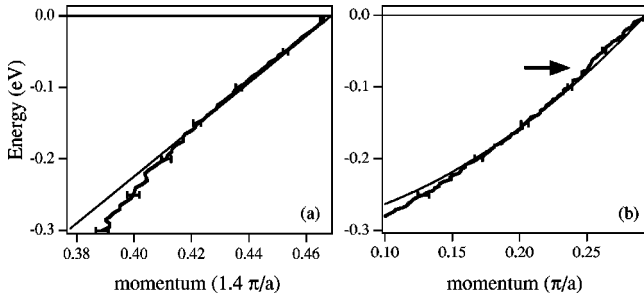
FIG. 4. Dispersions fitted from the spectral function analysis. (a) $\Gamma \rightarrow (\pi, \pi)$. The sharp upturn at low energies ($\omega < 15$ meV) is believed to be an artifact of the finite energy resolution. (b) $(\pi, 0) \rightarrow (\pi, \pi)$. The smooth lines are simple fits [linear and parabolic for (a) and (b), respectively]. The horizontal bars represent the uncertainty in the peak position from the Lorentzian fits. The arrow marks the position of the low-energy kink.

the fact that for straightforward electron-boson coupling one expects that the dispersion recovers to the bare one within about 5 times the bosonic band width. In the $(\pi, 0)$ region of the BZ, the local bare electronic band width may be narrower than this bosonic bound, so one has to regain a parabolic dispersion more quickly.

We note that finite resolution effects should not cause an inaccurate parametrization except very close to the Fermi energy. Close to E_F where the Fermi function differs significantly from unity, finite energy resolution (ΔE) weights the signal at each individual ω point disproportionately towards higher energy so that only fits to ω higher than ΔE are reliable and intrinsic. The sharp change to higher velocity at $\omega < 15$ meV in the Γ to (π, π) direction is obviously explained by effects of this kind. As will be shown later, the data from this energy region show also a sharp decrease in scattering rate along the zone diagonal. We consider this also to be an artifact of finite energy resolution, although the reason such an effect does not show up in the $(\pi, 0)$ to (π, π) direction is an open question.

As detailed above, the widths of the MDC Lorentzians can be parametrized as $\Sigma''(\vec{k}, \omega)/\vec{v}_F^{\,0}$. Like the case of λ', in
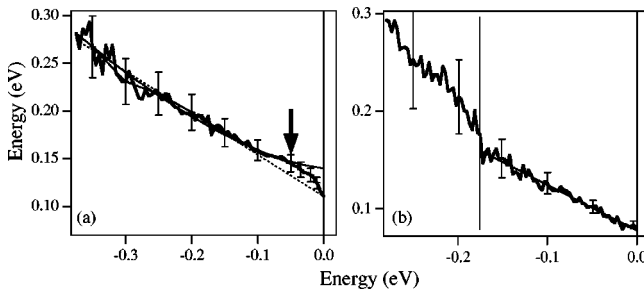

FIG. 5. Energy widths Σ'' as fitted from spectral function MDC's and multiplied by velocity. (a) $\Gamma \rightarrow (\pi, \pi)$. The solid line and dashed line are power-law fits [$\Sigma''(\omega) = \Sigma''(0) + A\omega^\alpha$] with $\alpha = 1.55$ and 1, respectively. The arrow marks the point of low-energy drop in Σ''. (b) $(\pi, 0) \rightarrow (\pi, \pi)$. The solid line is a linear fit. The vertical bar at 0.18 eV marks the energy beyond which the MDC width fits are not reliable. Vertical error bars represent the uncertainty in the fitted Lorentzian width.

the absence of a definitive independent measure for $\vec{v}_F^{\,0}$, we use for $\vec{v}_F^{\,0eff}$ the $\vec{v}$ from a $\omega \rightarrow 0$ extrapolation of a fit to the higher-energy dispersion to get a rough estimate for Σ''. For instance, in the $(\pi, 0)$-(π, π) direction, we use the value for the $\vec{v}_F^{\,0}$ of the fitted parabola. This fit, although displayed as extrapolated to $\omega = 0$, does not use input data for $\omega < 100$ meV.

Along the Γ-(π, π) direction [Fig. 5(a)], $\Sigma''(\omega)$ is best fit (solid line) in the higher-energy region (0.4 eV$> \omega$ >0.09 eV) to a power law form, $\Sigma''(\omega) = \Sigma''(0) + A\omega^\alpha$, with $\Sigma''(0) = 0.14$ eV and $\alpha = 1.55$. Note, that the best fit to a linear dependence (dashed line) with a $\Sigma''(0)$ of 0.11 eV does not fit nearly as well. We observe a low-energy drop in Σ'' at ≈ 0.07 eV. Although the drop is subtle, we believe the effect to be intrinsic as it was seen in a number of samples and is outside the uncertainty in the fits as represented by the error bars. Note that this is close to the same energy that the mass renormalization is found at in the $(\pi, 0)$-(π, π) direction. The precipitous drop in Σ'' for $\omega < 15$ meV is found from fitted MDC's that gave the artificial upturn in the dispersion in Fig. 4(a) and therefore appears to be an artifact of finite energy resolution.

In contrast, along the $(\pi, 0)$-(π, π) direction, $\Sigma''(\omega)$ is best fit by a linear dependence on ω, with $\Sigma''(0) = 0.08$ eV, with no signature of a low-ω drop in the scattering rate. Note that due to the much smaller local electronic band width in this region of the BZ, the MDC Lorentzian fit breaks down at energies higher than ≈ 0.2 eV as may have been expected from a visual inspection of Fig. 1(c). It is interesting to note that $\Sigma''(0)$, extracted in this way, is very different for the two directions. Also note that the finite energy (ΔE) and momentum resolution ($\Delta \vec{k}$) only give a minor broadening contribution to Σ'' as $\Delta \Sigma'' = \sqrt{(\partial E_{\vec{k}}/\partial \vec{k} \cdot \Delta \vec{k})^2 + (\Delta E)^2} \approx 28$ meV.

IV. DISCUSSION

As discussed above and in Ref. 10, due to its ubiquity, temperature dependence, and energy scale, the strong velocity renormalizations in the p-type materials has been attributed to an interaction of the charge carriers with phononic degrees of freedom. In the n-type compounds, we see some evidence of similar effects although important differences exist. As detailed above, there is no kink along the zone diagonal, which is the region of the BZ that shows the most unambiguous effect in the hole doped materials. There does appear to be a kink along the $(\pi, 0)$ to (π, π) direction. However, as we will discuss below, the interpretation of this feature is not straightforward.

If there exists a symmetry reducing order (or associated fluctuations) with characteristic wave vector (π, π), then one may expect to see two features in the EDC's in portions of the BZ where the unreconstructed band structure is below E_F in momentum regions straddling both sides of the antiferromagnetic BZ boundary since the effect of such an order is to reflect features across the antiferromagnetic BZ boundary, i.e., spectral features from (h, k) would be expected to show up at $(-h + \pi, -k + \pi)$. For instance, EDC's from

near the Fermi surface near $(\pi,0.3\pi)$, would have features reflective of the unreconstructed bands well below E_F from near $(0.7\pi,0)$. In contrast, EDC's from the band near $(0.45\pi,0.45\pi)$ will not have features that derive from near $(0.55\pi,0.55\pi)$ as this region of the BZ in the unreconstructed band structure is well above E_F. In this way, such a BZ reducing order may be expected to greatly modify the spectral function near $(\pi,0)$, but not as much near $(\pi/2,\pi/2)$ for an unreconstructed holelike Fermi surface centered at (π,π). Two such features in the EDC can give a kink in the effective dispersion if an MDC analysis is performed. As it has been previously noted that there are two features in the EDC's near the $(\pi,0)$ position[18,19,22] [see Fig. 2(b)] and there is evidence for fluctuations of some kind of (π,π) symmetry reducing order, we do not believe that there is sufficient evidence to unambiguously assign the $(\pi,0)$-(π,π) kink feature, found by an MDC analysis, the same origin as the kink observed in the p-type compounds. We believe there is no means to unambiguously separate the (π,π) symmetry reducing effect. In this regard, the kink found along $(\pi,0)$-(π,π) in the present work appears to be of a different sort than the zone diagonal kink found in the p type. The current case may be an example of a mass renormalization due to the effects of generic residual antiferromagnetism (i.e., not a resonance mode) or other symmetry reducing order with characteristic wave vector (π,π) and therefore its observation does not directly bear on the debate regarding the relative merits of the phonon vs magnetic resonance mode scenarios for the spectral function of the cuprates.

Despite the uncertainties in the MDC analysis, one can make a strong statement about the lack of a kink along the zone diagonal. By the same condition as given above, in this region of the BZ, we do not expect to see (π,π) features (nor are any observed) as the unreconstructed Fermi sea is only filled on one side of antiferromagnetic BZ boundary. Visual inspection of the MDC fitted dispersion in the 0.2 eV$>\omega>0$ eV range shows there no feature resembling a sharp kink in the dispersion.[24]

The dependence of the scattering rate on frequency along the zone diagonal is different from the linear dependence reported in the optimally doped p-type materials[25] (note that some groups have found possible deviations from linear[26]). This stronger $\omega^{1.55}$ dependence in the electron doped compounds compares more closely to the quadratic temperature dependence of their resistivity than to the linear temperature dependence of the hole doped materials at optimal doping.[27,28]

Our results for Σ'' may also be compared to the linear dependence of the low-energy (>1000 cm^{-1}) scattering rate that has been found by an inversion of the optical conductivity.[29,30] The conventional wisdom is that zone diagonal states give the primary contribution to transport due to their supposedly higher $\vec{v}_F$. At first glance this is not consistent with our finding here. However, as we have found for the electron doped material that the $\vec{v}_F$ at the Γ-(π,π) FS crossing is not greatly different from that found at the $(\pi,0)$-(π,π) FS crossing [this is another consequence of the

fact that the $(\pi,0)$ saddle point is ≈ 300 meV below E_F], the $(\pi,0)$ region (where a linear dependence is found) may contribute somewhat equally to the optical scattering rate. Moreover, as may be seen in Fig. 5(a), the scattering rate along the zone diagonal can be fit approximately by a linear dependence above 130 meV and it may be that it is this energy which is contributing the most to the optical excitations for $E_\gamma > 1000$ cm^{-1}(≈ 100 meV). Optical experiments also find a low-energy drop in the scattering rate below an energy (650 cm$^{-1} \approx 70$ meV) very close to that where we find the depression in Σ'' and a mass renormalization.[29,30]

The energy at which we observe the mass renormalization along the $(\pi,0)$ to (π,π) direction is the same energy to within experimental uncertainty, that we observe the drop in the scattering rate along Γ-(π,π). Although these energy scales are consistent with each other, this observation is inconsistent with Kramers-Kronig considerations. Since Σ' and Σ'' are real and imaginary components derived from the same response function, they should be related via a Kramers-Kronig transform due to causality. If Σ' along a particular cut shows a kink, then Σ'' should show a corresponding drop. The reason such a behavior is not observed is unclear, but may be related to momentum dependence in the self-energy masking such effects. If the self-energy is momentum dependent, the dispersion and width obtained from MDC analysis cannot be simply related to Σ' and Σ'', respectively. It does seem that the qualitative conclusion that there is little renormalization along the zone diagonal remains valid. The situation for the $(\pi,0)$-(π,π) direction is less clear, as the mass renormalization is present here and the situation to compare to in the p types near $(\pi,0)$ more uncertain.

As detailed above, it seems reasonable to associate the mass renormalization on the p-type side of the phase diagram with a strong coupling of charge carriers to phononic degrees of freedom. Specifically, the principal phonon has been conjectured[10] to be the oxygen half-breathing mode, which is seen to have anomalous softening and spectral weight changes in the relevant energy range near the doping induced metal-insulator transition as probed by neutron scattering.[31–34] A number of recent studies have found similar signatures of phononic anomalies in the electron doped materials.[35,36] Kang *et al.* found changes with doping in the generalized phonon density of states around ≈ 70 meV by neutron scattering. d'Astuto *et al.* measured phonon dispersions via inelastic x-ray scattering and assigned the softening they found in the 55–75 meV energy range to the same oxygen half-breathing mode that anomalies are found in in the p-type materials. These studies give evidence for phononic effects in the electron doped materials that are somewhat similar to those found in the hole doped compounds.

There are a number of differences that do exist in these anomalies that may provide a starting point for understanding why similar signatures in the boson spectrum may cause similar effects not to appear in ARPES. Although the biggest changes in the phonon density of states probed by Kang *et al.* happen at similar doping levels in La$_{2-x}$Sr$_x$CuO$_4$ and Nd$_{2-x}$Ce$_x$CuO$_4$($x\approx 0.04$), the doping levels are at very dif-

ferent relative positions in the phase diagram, with $x = 0.04$ being still well into the antiferromagnetic (and possibly more insulating) phase for the electron doped compound. As such modifications in the phonon spectrum may be associated generally with screening changes (and hence electron-phonon coupling) with the onset of metallicity, this demonstrates the possibility that the changes in the NCCO phonon spectrum, although superficially similar in the electron and hole doped materials, are in some sense different. d'Astuto *et al.* found that although the softening of the phonon dispersion appears in a somewhat similar way at a similar energy scale as in the *p*-type materials, differences do exist in the shape of the anomaly in the phonon dispersion. Moreover, on general grounds, since the purported soft phonon is the oxygen half-breathing mode, one may naively expect a weaker coupling for this mode with electron doping, as Madelung potential considerations[37] indicate that doped electrons will preferentially sit on the Cu site, whereas doped holes have primarily oxygen character.

Kang *et al.* have mentioned[35] that it would be interesting to look for mass renormalizations in the ARPES spectra of the *n*-type underdoped compounds that they first detect phonon anomalies in. However, we believe that if the electron-phonon coupling is of the same nature in the $n-$ and $p-$ type materials it should reveal itself in the ARPES spectra of the highest-T_c electron doped samples as it does in the hole doped materials. Moreover, the issue of looking for mass renormalizations and at peak widths may not even be relevant at the extremely low dopings ($x = 0.04$) where Kang *et al.* see the largest changes in the phonon density of states, as there are only regions of the BZ with enhanced near-E_F spectral weight and no well-defined electronic peaks.[38] The question of what the electron-phonon coupling parameter is as one enters the Mott insulating state at very low dopings may not even be particularly well posed, as the near-E_F spectral weight vanishes as $x = 0$ is approached.

V. CONCLUSION

A modern spectral function analysis reveals very different and likely weaker signatures of possible bosonic effects in the ARPES spectra of $Nd_{1.85}Ce_{0.15}CuO_4$ along the two main symmetry directions of the BZ as compared to the hole doped compounds. However, unlike the *p*-type compounds, we believe that one cannot distinguish the various contributions to the self-energy into separate effects, as the simple analysis yields results which are not consistent with Kramers-Kronig considerations. Despite the complexities inherent in assigning various features in the spectra to distinct sources, a direct comparison between the *p*- and *n*-type compounds does have utility, as we have shown the lack of a mass renormalization along the zone diagonal. Our analysis shows that whatever is causing the distinct effect in the hole doped materials manifests itself less strongly on the *n*-type side, perhaps due to a weaker electron-phonon coupling or masking effects from other interactions. Although such observations are consistent with a weaker electron-phonon coupling in the electron doped cuprates, a strong discrepancy exists between these measurements and a number of scattering studies that point to strong electron-phonon coupling. Perhaps, some of the intrinsic differences between electron and hole dopings may provide a route towards reconciling these different measurements and thereby giving insight into the underlying phenomenon.

[1] A. Damascelli, Z.-X. Shen, and Z. Hussain, Rev. Mod. Phys. **75**, 473 (2003).

[2] J.C. Campuzano, M.R. Norman, and M. Randeria, *Physics of Conventional and Unconventional Superconductors*, edited by K. H. Bennemann and J. B. Ketterson (Springer-Verlag, Berlin, 2002).

[3] S. Hüfner, *Photoelectron Spectroscopy: Principles and Application* (Springer-Verlag, New York, 1995).

[4] We should note that this analysis is predicated on the fact that it is physically reasonable to express interaction effects as *electronic* self-energies. In this sense, the marginal Fermi liquid phenomenology (Ref. 5) may represent a "worst case" scenario in assigning physical meaning to such self-energies. If, in fact, the cuprates are non-Fermi liquids in the sense that the fundamental excitations have integrity that are distinct from electrons, this analysis may not be valid. Indeed, in such a case or in any case where the MDC's are not well represented as Lorentzians, this analysis will cause an inaccurate and unphysical parametrization of the spectra.

[5] C.M. Varma, P.B. Littlewood, S. SchmittRink, E. Abrahams, and A.E. Ruckenstein, Phys. Rev. Lett. **63**, 1996 (1989).

[6] M. Hengsberger, D. Purdie, P. Segovia, M. Garnier, and Y. Baer, Phys. Rev. Lett. **83**, 592 (1999).

[7] S. Lashell, E. Jensen, and T. Balasubramanian, Phys. Rev. B **61**, 2371 (2000).

[8] T. Valla, A.V. Fedorov, P.D. Johnson, and S.L. Hulbert, Phys. Rev.

Lett. **83**, 2085 (1999).

[9] P.V. Bogdanov, A. Lanzara, S.A. Kellar, X.J. Zhou, E.D. Lu, W.J. Zheng, G. Gu, J.-I. Shimoyama, K. Kishio, H. Ikeda, R. Yoshizaki, Z. Hussain, and Z.X. Shen, Phys. Rev. Lett. **85**, 2581 (2000).

[10] A. Lanzara, P.V. Bogdanov, X.J. Zhou, S.A. Kellar, D.L. Feng, E.D. Lu, T. Yoshida, H. Eisaki, A. Fujimori, K. Kishio, J.-I. Shimoyama, T. Noda, S. Uchida, Z. Hussain, and Z.-X. Shen, Nature (London) **412**, 510 (2001).

[11] A. Kaminski, M. Randeria, J.C. Campuzano, M.R. Norman, H. Fretwell, J. Mesot, T. Sato, T. Takahashi, and K. Kadowaki, Phys. Rev. Lett. **86**, 1070 (2001).

[12] P.D. Johnson, T. Valla, A.V. Fedorov, Z. Yusof, B.O. Wells, Q. Li, A.R. Moodenbaugh, G.D. Gu, N. Koshizuka, C. Kendziora, Sha Jian, and D.G. Hinks, Phys. Rev. Lett. **87**, 177007 (2001).

[13] A. D. Gromko, A. V. Fedorov, Y.-D. Chuang, J. D. Koralek, Y. Aiura, Y. Yamaguchi, K. Oka, Yoichi Ando, and D. S. Dessau, cond-mat/0202329 (unpublished).

[14] Hae-Young Kee, Steven A. Kivelson, and G. Aeppli, Phys. Rev. Lett. **88**, 257002 (2002).

[15] Ar. Abanov, A.V. Chubukov, M. Eschrig, M.R. Norman, and J. Schmalian, Phys. Rev. Lett. **89**, 177002 (2002).

[16] See, for instance, Sudip Chakravarty, R.B. Laughlin, Dirk K. Morr, and Chetan Nayak, Phys. Rev. B **63**, 094503 (2001).

[17] Y. Tokura, H. Takagi, and S. Uchida, Nature (London) **337**, 345 (1989).

[18] N.P. Armitage, D.H. Lu, C. Kim, A. Damascelli, K.M. Shen, F. Ronning, D.L. Feng, P. Bogdanov, Z.-X. Shen, Y. Onose, Y. Taguchi, Y. Tokura, P.K. Mang, N. Kaneko, and M. Greven, Phys. Rev. Lett. **87**, 147003 (2001).

[19] N.P. Armitage, D.H. Lu, D.L. Feng, C. Kim, A. Damascelli, K.M. Shen, F. Ronning, Z.-X. Shen, Y. Onose, Y. Taguchi, and Y. Tokura, Phys. Rev. Lett. **86**, 1126 (2001).

[20] K. Yamada, K. Kurahashi, T. Uefufi, M. Fujita, S. Park, S.-H. Lee, and Y. Endoh, Phys. Rev. Lett. **90**, 137004 (2003).

[21] Data consistent with those presented here were also obtained on samples where the reducing condition was 100 h in flowing argon gas at 1000 °C.

[22] T. Sato, T. Kamiyama, T. Takahashi, K. Kurahashi, and K. Yamada, Science **291**, 1517 (2001).

[23] These values for λ' are in actuality an upper bound on the full renormalization as there is no independent measure of the bare dispersion to get $\vec{v}_F^0$.

[24] The slight negative curvature in the dispersion found along the zone diagonal is due to the MDC fits becoming less reliable at higher energies. A fit using EDC's at high energy reveals the expected positive curvature.

[25] T. Valla, A.V. Fedorov, P.D. Johnson, B.O. Wells, S.L. Hulbert, Q. Li, G.D. Gu, and N. Koshizuka, Science **285**, 2110 (1999).

[26] X. J. Zhou (unpublished).

[27] F. Gollnik and M. Naito, Phys. Rev. B **58**, 11 734 (1998).

[28] Y. Onose, Y. Taguchi, K. Ishizaka, and Y. Tokura, Phys. Rev. Lett. **87**, 217001 (2001).

[29] C.C. Homes, B.P. Clayman, J.L. Peng, and R.L. Greene, Phys. Rev. B **56**, 5525 (1997).

[30] E.J. Singley, D.N. Basov, K. Kurahashi, T. Uefuji, and K. Yamada, Phys. Rev. B **64**, 224503 (2001).

[31] R.J. McQueeney, Y. Petrov, T. Egami, M. Yethiraj, G. Shirane, and Y. Endoh, Phys. Rev. Lett. **82**, 628 (1999).

[32] R.J. McQueeney, J.L. Sarrao, P.G. Pagliuso, P.W. Stephens, and R. Osborn, Phys. Rev. Lett. **87**, 077001 (2001).

[33] L. Pintschovius and M. Braden, Phys. Rev. B **60**, R15 039 (1999).

[34] Y. Petrov, T. Egami, R. J. McQueeney, M. Yethiraj, H. A. Mook, and F. Dogan, cond-mat/0003414 (unpublished).

[35] H.J. Kang, Pengcheng Dai, D. Mandrus, R. Jin, H.A. Mook, D.T. Adroja, S.M. Bennington, S.-H. Lee, and J.W. Lynn, Phys. Rev. B **66**, 064506 (2002).

[36] M. d'Astuto, P.K. Mang, P. Giura, A. Shukla, P. Ghigna, A. Mirone, M. Braden, M. Greven, M. Krisch, and F. Sette, Phys. Rev. Lett. **88**, 167002 (2002).

[37] J.B. Torrance and R.M. Metzger, Phys. Rev. Lett. **63**, 1515 (1989).

[38] N.P. Armitage, F. Ronning, D.H. Lu, C. Kim, A. Damascelli, K.M. Shen, D.L. Feng, H. Eisaki, Z.-X. Shen, P.K. Mang, N. Kaneko, M. Greven, Y. Onose, Y. Taguchi, and Y. Tokura, Phys. Rev. Lett. **88**, 257001 (2002).